Beam test of a one-dimensional position sensitive chamber on synchrotron radiation *

LIU Mei(刘梅)[1,3,4;1)] DAI Hong-Liang(代洪亮)[1,3] QI Hui-Rong(祁辉荣)[1,3;2)] ZHUANG Bao-An(庄保安)[1,3]
ZHANG Jian(张建)[1,3] LIU Rong-Guang(刘荣光)[1,3] ZHU Qi-Ming(朱启明)[1,3]
OUYANG Qun(欧阳群)[1,3] CHEN Yuan-Bo(陈元柏)[1,3] JIANG Xiao-Shan(江晓山)[1,3]
WANG Ya-Jie(王雅洁)[2,3] LIU Peng(刘鹏)[3] CHANG Guang-Cai(常广才)[3]

[1] State Key Laboratory of Particle Detection and Electronics, Beijing 100049, China
[2] CAS Key Laboratory for Biological Effects of Nanomaterials and Nanosafety, Beijing 100049, China
[3] Institute of High Energy Physics, Chinese Academy of Sciemces, Beijing 100049, China
[4] University of Chinese Academy of Sciences, Beijing 100049, China

Abstract: A one-dimensional single-wire chamber was developed to provide high position resolution for powder diffraction experiments with synchrotron radiation. A diffraction test using the sample of SiO_2 has been accomplished at 1W2B laboratory of Beijing Synchrotron Radiation Source. The data of the beam test were analyzed and some diffraction angles were obtained. The experimental results were in good agreement with standard data from ICDD powder diffraction file. The precision of diffraction angles was 1% to 4.7%. Most of the relative errors between measured values of diffraction angles and existing data were less than 1%. As for the detector, the best position resolution in the test was 138 μm (σ value) with an X-ray tube. Finally, discussions of the results were given. The major factor that affected the precision of measurement was deviation from the flat structure of the detector. The effect was analyzed and the conclusion was reached that it would be the optimal measurement scheme when the distance between the powder sample and detector was from 400 mm to 600 mm.

Key words: gaseous detector, synchrotron radiation, powder X-ray diffraction, ICDD-pdf

PACS: 29.40.Cs, 29.20.dk **DOI:** 10.1088/1674-1137/37/10/108001

1 Introduction

Since the advent of MWPC by Charpak [1], wire chambers have been widely used in high energy physics experiments. They can, for example, provide high precision measurement when working as part of the time expansion chamber system in TWIST experiment [2]. In the last few years, wire chambers are frequently applied to neutron detection because of their low-cost, large-area and reliability [3]. X-ray diffraction is an irreplaceable method for powder crystal lattice measurement. Meanwhile, synchrotron light sources provide intense, tunable and highly collimated radiation which covers from microwaves to hard X-rays. The pulsed time structure in synchrotron X-ray makes it suitable to be applied to biological macromolecule measurement, usually with 0.5–2 X wavelength [4]. Wire chambers have been used for diffracted X-ray detection. A one dimensional curved wire chamber with delay line readout has been constructed for use in powder X-ray crystallography [5]. With the same objective, in our case, the detector design was improved for higher performance. A single-wire chamber with an FPGA chip was built for powder X-ray diffraction detection. The detector has been used on Synchrotron Radiation X-ray beam. In the paper, results are presented and well discussed. The results display a positive attitude toward applying one-dimensional wire chambers to SR X-ray diffraction experiment.

2 Principle of operation and experimental setup

2.1 Principle of X-ray diffraction

When the parallel X-ray irradiates an SiO_2 powder sample, it produces diffraction at certain angles. The angles are determined by Bragg's law:

$$2d\sin\theta=\lambda, \quad (1)$$

Received 19 November 2012, Revised 21 December 2012
* Supported by National Natural Science Foundation of China (11275224)
1) E-mail: lium@ihep.ac.cn
2) E-mail: qihr@ihep.ac.cn

where 2θ is the angle between the diffracted and incident directions. Due to the isotropy of the powder, the diffracted X-ray will form a series of cones at 2θ directions. When using a 2D imaging detector, there would be several bright rings on the receiving plane. As for a 1D wire chamber, it would detect a series of symmetrical points along x axis [6].

2.2 One-dimensional wire chamber detector

The wire chamber is made up of an entrance window (along with an upper cathode), an anode wire, a readout pad and the following electronics, seen in Fig. 1. The sensible volume of the detector is 200 mm×50 mm×8 mm, as the effective detection length is 20 cm. The entrance window is 200 mm×10 mm in area, made of 55 μm thick Al foil. The upper cathode is made of the same foil but with bigger size. The anode wire is 15 μm gold plated tungsten. Under the wire, 200 strips on the readout pad are 0.5 mm wide and at 0.5 mm intervals. The chamber is filled with gas, which is usually the mixture of 70% argon and 30% carbon dioxide. Gas pressure is maintained at 1 atm. The upper cathode and readout pad are at zero potential, while the anode wire is maintained at high voltage.

When an X-ray photon hits the detector, signals are induced on both anode wire and some readout strips. Induced signals are amplified by AMP before being discriminated. The pulse width of discriminated signals is proportional to Q value. Discriminated signals will be transferred to FPGA, which handles a fast processing of signals. In particular, TDC in FPGA will convert signals into digital codes. According to the corresponding wire number, the centroid method will be used on the digital signals. As a result, the barycenter position of the hit is fixed. Hit position information of the photon will be recorded into a data file and delivered to the computer (Fig. 2).

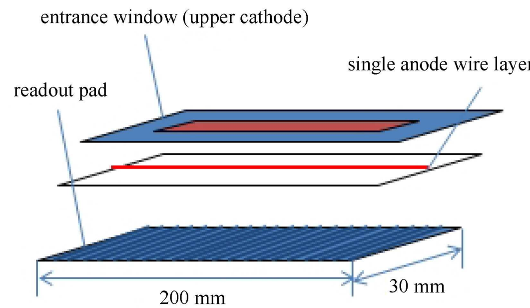

Fig. 1. A schematic picture showing 1D single-wire chamber structure, the gap between neighboring layers is 4 mm.

The position resolution of the detector affects the precision of the diffraction angles. An experiment for its measurement was set up with an X-ray machine. The X-ray passed through a 20 μm slit before it hit the detector. With 1520V voltage and 90%Ar+10%CO_2 gas, the best position resolution measured was 138 μm in σ (Fig. 3(a)). The voltage was set according to counting rate plateau (Fig. 3(b)).

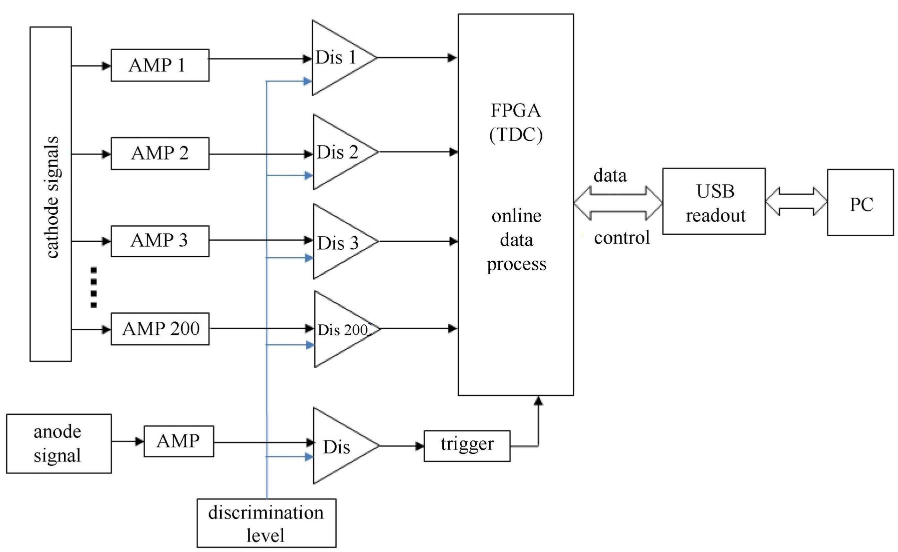

Fig. 2. The signal readout electronics of the detector.

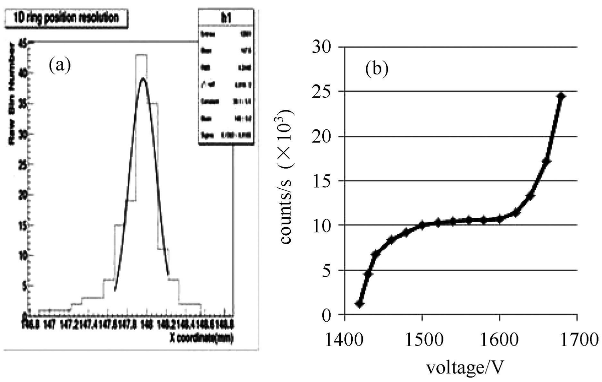

Fig. 3. (a) Position resolution with 20 μm slit@ Ar/CO_2(90/10); (b) Count rate with high voltage@Ar/CO_2(90/10).

2.3 Experimental setup on SR X-ray beam

At 1W2B laboratory of SR Source, the experimental setup for testing is shown in Fig. 4. The beam piping, slit, SiO_2 sample and detector are at the same height with a common X axis center. The lead block is arranged for the protection of the detector. It is assumed that incident direction is Z and the detector is installed along X. The parallel synchrotron X-ray from a small piping irradiated the SiO_2 sample and produced diffraction. The diffracted X-ray was detected by a single-wire chamber in front. The energy of the X-ray changed from 12 keV to 19 keV, as well as the distance between SiO_2 sample and detector varying from 200.5 mm to 232.5 mm. The powder SiO_2 used in the test is a standard sample which is NO, 46-1045 in the powder diffraction file-2 (pdf-2), The International Centre for Diffraction Data (ICDD).

According to Bragg's law, the interplanar spacing d is determined by diffraction angle 2θ with a given wavelength. In that case, the accuracy of measured d depends on the accuracy of measured 2θ. In this test, X-ray wavelength is given, which means the measurement of diffraction angles is of most concern.

3 Results and discussion

3.1 Test results

During the SR beam test, two parameters have been changed: the energy of X-ray (E) and the distance between SiO_2 sample and the detector (S).

When online data acquisition was done, raw data files were obtained on PC. Each file contained 12800 counts, and the data obeyed Gaussian distribution at some specific area. Offline data processing was accomplished by ROOT [7] software. Since the diffraction peaks were symmetric about y axis, only the $+x$ data was processed. The diffraction peak position (l) information was achieved by applying Gaussian Fitting. Diffraction angles were worked out using trigonometric function:

$$2\theta=\arctan\left(\frac{l}{S}\right). \tag{2}$$

Assuming S is accurate, according to error transfer formula:

$$N=f(x),\quad \sigma_{\rm N}=\frac{\partial f}{\partial x}\cdot\sigma_x. \tag{3}$$

It can be deduced that:

$$\sigma_{2\theta}=\frac{S\cdot\sigma_l}{S^2+l^2}, \tag{4}$$

σ_l is the standard deviation of l obtained from Gaussian Fitting.

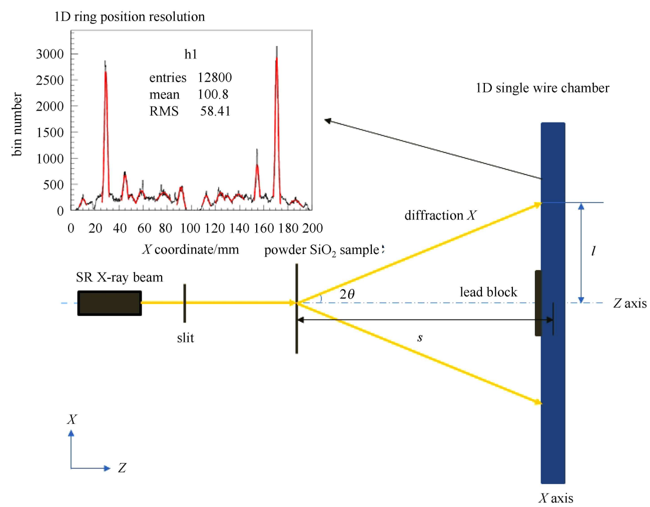

Fig. 4. A schematic diagram of diffraction experimental setup on SR X-ray beam. The spectrum shows 1D diffraction peaks of the sample.

ICDD has provided standard d values, as well as 2θ values with a given X-ray wavelength. Fig. 5 and Fig. 6 presented 2θ values coming from the experiment and ICDD pdf-2 [8]. The differences between them were measurement errors. The error bars ($\sigma_{2\theta}$) on the experimental data represented precision of measurement. According to the data, most of the relative errors between measured values and standard values were <1%, while the precision of measured values was 1%–4.7%. If one only cares about the strongest diffraction peak, the precision can be raised to 1%–3%. When 2θ values converted into d values, relative errors were also <1%.

3.2 Discussion

The measurement errors on the diffraction angles have met expectation; what we focused on is improving the precision of measurement. The source of deviation and its correction were analyzed. Deviation could come from experimental method, which can't be eliminated. Fig. 7 showed two kinds of deviation originating from

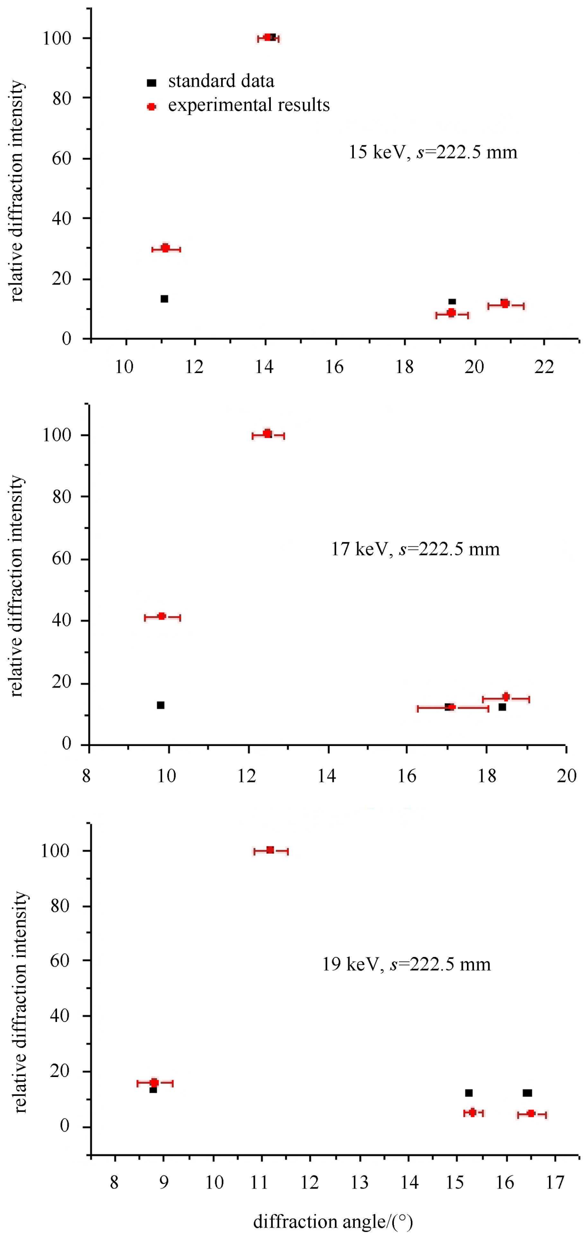

Fig. 5. (color online) Diffraction angle of sample at various energy (red points are experimental 2θ, black squares are pdf-2 standard data).

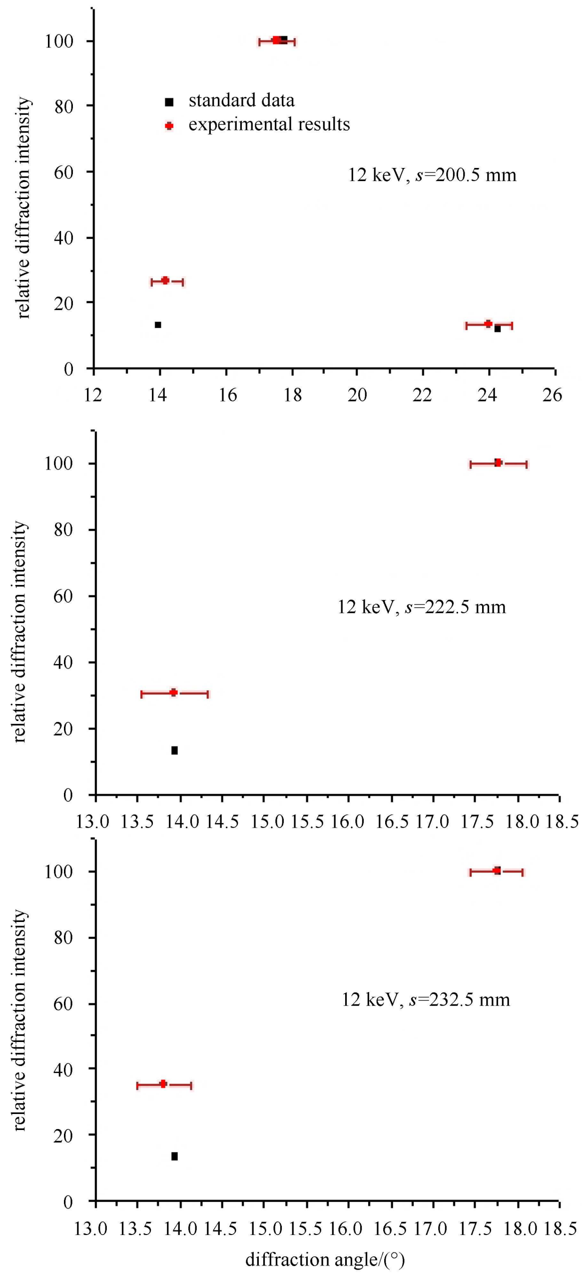

Fig. 6. (color online) Diffraction angle of sample at different distances (red points are experimental 2θ, black squares are pdf-2 standard data).

the structure of the detector. In the former, the flat construction of the detector caused imaging aberration $r_{\rm a}$:

$$r_{\rm a}=h\cdot\tan2\theta,\quad h=8\ \text{mm}, \tag{5}$$

as the detector was 8 mm thick in Z direction. In the latter, the width of the detection in y axis caused detection deviation $r_{\rm b}$:

$$r_{\rm b}=l-\sqrt{l^2-\left(\frac{y}{2}\right)^2},\quad l=s\cdot\tan2\theta, \tag{6}$$

where y is the width of the entrance window with 10 mm. It might be noted that $r_{\rm a}$ and $r_{\rm b}$ always have the different signs. $r_{\rm b}$ is confirmed to be negligible, while $r_{\rm a}$ causes deviation on the position of diffraction peaks, resulting in damage on 2θ position resolution. Assuming the hitting events are equally distributed within $r_{\rm a}$ area, the deviation (σ_r) caused by it is $r_{\rm a}/\sqrt{12}$. As it was found in the experiment that 2θ precision is enhanced as 2θ increases, in the case of 12 keV X-ray, we only consider the minimum diffraction angle. Table 1 shows to what extent r_a affects the final standard deviation on 2θ angles. Although relative $\sigma_{2\theta}$ decreases with increasing S, ratio $\sigma^r_{2\theta}/\sigma_{2\theta}$ rises.

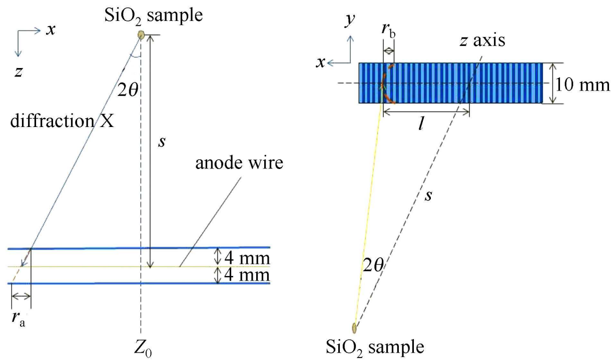

Fig. 7. (a)The plain receiving surface of the detector produced maximum position error r_a on x axis; (b) The 30 mm length of readout strips on y axis produced maximum position error r_b.

Table 1. Representation of relative $\sigma_{2\theta}$ and relative $\sigma^r_{2\theta}$ on experiment and calculation.

S/mm	experimental relative $\sigma_{2\theta}$	calculated relative $\sigma^r_{2\theta}$	$\sigma^r_{2\theta}/\sigma_{2\theta}$
200.5	3.27%	1.11%	33.8%
222.5	2.57%	1.00%	38.8%
232.5	2.20%	0.95%	43.3%
300		0.74%	
400		0.55%	
500		0.44%	
600		0.37%	
700		0.32%	

When S=400 mm, it can be deduced that $\sigma^r_{2\theta}/\sigma_{2\theta}>$ 50%. Based on the expected relative $\sigma^r_{2\theta}$ value, it makes corresponding $\sigma_{2\theta}<1\%$, which is the expectation of further measurement.

In spite of the fact that diffraction angles acquire higher precision with longer S, the beam intensity would limit the longest distance. For 8 keV X-ray, the mass attenuation coefficient for air is 9.9 cm^2/g(18 °C, [9]). It can be deduced that the intensity of X-ray would be attenuated to ∼50% at the distance of 600 mm, which defines the limit. In conclusion, to improve the precision of measurement without damaging detection efficiency, an optimal scheme proposed is to keep the distance S between 400–600 mm.

4 Conclusion

A one-dimensional position sensitive detector has been developed with 200 readouts and ⩾138 μm position resolution ratio. Measurement of X-ray diffraction with this detector has been accomplished on synchrotron radiation source. Some results have been obtained. The diffraction angles in the experiment were in accordance with standard data. In particular, the relative errors between experimental results and standard data were <1%. The precision of measured angles was 1% to 4.7%. An optimized solution is proposed for improvement, that is, confining the distance between the sample and detector to 40–60 cm. This would raise the precision to <1%.

The experiment indicates that a single chamber could be used on the measurements of X-ray diffraction on SR source. Moreover, compared to the existing X-ray diffractometers, the 1D single-wire chamber has equal precision but simpler structure and larger measuring range. Finally, its cheap cost makes it more practical. The further plan on the test is measuring diffraction angles with the improved scheme, while changing the kind of working gas, as well as the kind of powder sample, such as ZnO.

We gratefully acknowledge the contributions of all members at 1W2B laboratory of Beijing Synchrotron Radiation Source and we appreciate WANG Ya-jie for preparation of the samples.

References

1 Charpak G et al. Nucl. Instrum. Methods, 1968, **62**: 262–268
2 HU J, Sheffer G, Davydov Y I et al. Nucl. Instrum. Methods A, 2006, **566**: 563–574
3 Bleif H K, Clemens D, Eads A et al. Nucl. Instrum. Methods A, 2007, **580**: 1110–1114
4 Helliwell J R et al. Nucl. Instrum. Methods, 1982, **201**: 175–180
5 Ortendahl D et al. Nucl. Instrum. Methods, 1978, **156**: 53–56
6 Jenkins R. X-ray Fluorescence Spectrometry. Version 2. Published in: John Wiley & Sons, Inc., 2012. 37
7 ROOT, http://root.cern.ch/drupal/
8 PDF-ICDD Powder Diffraction File - 2 (Set 46-1045), International Centre for Diffraction Data, Newtown Square, PA, USA, 2006
9 NIST, http://www.nist.gov/pml/data/xraycoef/